Research in Astronomy and Astrophysics, 26:112001 (14pp), 2026 November
https://doi.org/10.1088/1674-4527/ae67a0
CSTR: 32081.14.RAA.ae67a0
© 2026. National Astronomical Observatories, CAS and IOP Publishing Ltd. All rights, including for text and data mining, AI training, and similar technologies, are reserved. Printed in China.

Ultra-compact X-Ray Binaries: A Review

Bo Wang[1], Dongdong Liu[1], Yunlang Guo[2], Hailiang Chen[1], Wen-Cong Chen[3], and Zhanwen Han[1]
[1] International Center of Supernovae (ICESUN), Yunnan Key Laboratory of Supernova Research, Yunnan Observatories, Chinese Academy of Sciences, Kunming 650216, China; wangbo@ynao.ac.cn, liudongdong@ynao.ac.cn
[2] School of Astronomy and Space Science, Nanjing University, Nanjing 210023, China; yunlang@nju.edu.cn
[3] School of Science, Qingdao University of Technology, Qingdao 266525, China
Received 2026 March 23; revised 2026 April 27; accepted 2026 April 30; published 2026 June 5

Abstract

Ultra-compact X-ray binaries (UCXBs) are a subclass of low-mass X-ray binaries (LMXBs) characterized by ultra-short orbital periods, typically less than 60−80 minutes. They consist of a compact mass-accretor and a hydrogen-poor mass-donor, in which the mass-accretor could be a neutron star (NS) or even a black hole (BH). UCXBs play an important role in multiple areas of astrophysics. In particular, they are considered strong, continuous gravitational wave (GW) sources in the low-frequency band, making them key targets for future space-based GW observatories such as LISA, TianQin and Taiji. As the most compact binaries, the formation and evolution of UCXBs remain highly uncertain. In this article, we summarize theoretical advances and observational status in UCXBs. Especially, we review four classic formation channels: the white dwarf donor channel, the He star donor channel, the evolved main-sequence donor channel, and the accretion-induced collapse channel. We also discuss recent progress in these channels, covering evolutionary scenarios, the initial parameter space of the progenitors, and associated objects. A comparison between observations and theoretical predictions is provided, along with a discussion on the observed BH-UCXB candidates and their formation path. The origin of UCXBs can be constrained by the chemical composition of mass-donors and their locations in diagrams of mass-transfer rate (or X-ray luminosity) versus orbital period. We also examine the implications of UCXBs for several astrophysical fields, including GW astronomy, multi-messenger astronomy, binary evolution, and NS physics under extreme conditions. Further progress will depend on multi-wavelength observations, the discovery of more samples, and more detailed theoretical simulations.

Key words: Stars – (stars:) binaries (including multiple): close – X-rays: binaries

1. Introduction

Low-mass X-ray binaries (LMXBs) are a type of mass-accretion powered X-ray sources, in which the mass-accretor could be a neutron star (NS) or a stellar-mass black hole (BH) that is accreting matter from a low-mass ($<1\,M_{\odot}$) companion through Roche-lobe overflow (RLOF; see Bhattacharya & van den Heuvel 1991; Tauris & Savonije 1999; Podsiadlowski et al. 2002). Binary millisecond pulsars (MSP) were generally thought to evolve from NS-LMXBs, in which an NS is spun up to millisecond periods by accreting matter and angular momentum from a low-mass donor (see, e.g., Alpar et al. 1982; Bhattacharya & van den Heuvel 1991). A few hundred LMXBs have been observed in the Galaxy, containing both transients and persistent sources (e.g., Liu et al. 2007; Casares et al. 2017).

Ultra-compact X-ray binaries (UCXBs) are a subclass of LMXBs with ultra-short orbital periods that are usually less than 60−80 minutes, consisting of a compact mass-accretor and a hydrogen-poor mass-donor (see Rappaport et al. 1982; Savonije et al. 1986; Nelson et al. 1986; Nelemans & Jonker 2010). Another kind of interacting ultra-compact binary is AM CVn systems, which have similar mass-donors as UCXBs but the mass-accretors are white dwarfs (WDs; see Warner 1995; Podsiadlowski et al. 2003a; Nelemans & Jonker 2010; Solheim 2010; Liu et al. 2021; Chen et al. 2022a; Green et al. 2025; Yu et al. 2026b).

UCXBs play a key role in modern astrophysics, as follows: (1) UCXBs are important low-frequency gravitational wave (GW) sources due to their short orbital periods, which can be detected by space-based GW detectors, such as LISA (e.g., Nelemans 2009; Amaro-Seoane et al. 2017; Tauris 2018; Amaro-Seoane et al. 2023), TianQin (e.g., Luo et al. 2016; Bao et al. 2019; Huang et al. 2020; Li et al. 2025a), and Taiji (e.g., Ruan et al. 2020, 2021). Meanwhile, UCXBs are also dual-band GW sources that can be potentially used to constrain the properties of NSs (see, e.g., Bildsten 1998; Suvorov 2021; Chen 2021). (2) In addition to GW radiation, UCXBs also emit X-ray and optical radiation simultaneously, and especially exhibit radio radiation in their late stages. This allows for simultaneous multi-wavelength observations, which is of great significance for the study of multi-messenger astronomy. (3) UCXBs are important astrophysical labs owing to the

Table 1
Catalog of 22 Confirmed UCXBs, Listing key Parameters Including the Orbital Period ($P_{\rm orb}$), the Spin Period ($P_{\rm spin}$), the Unabsorbed Peak X-ray Flux ($F_{\rm X}$[2–10 keV]), the Estimated Average Mass-transfer Rate ($\dot{M}_{\rm tr}$), the Companion Mass ($M_{\rm c}$), the Composition, the Distance (d) and the Location

Object	$P_{\rm orb}$ (min)	$P_{\rm spin}$ (ms)	$F_{\rm X}$[2–10 keV] (erg cm^{-2} s^{-1})	$\dot{M}_{\rm tr}$ ($M_\odot$ yr^{-1})	$M_{\rm c}$ ($M_\odot$)	Composition	d (kpc)	Location	References
Transient sources									
XTE J1807-294	40.1	5.25	1.19×10^{-10}	$<1.9^{+2.6}_{-1.6} \times 10^{-11}$	0.022	⋯	$8^{+4}_{-3.3}$	Bulge	(1), (2), (3)
XTE J1751-305	42.4	2.30	1.27×10^{-9}	$5.1^{+2.6}_{-2.9} \times 10^{-12}$	0.02	⋯	$8^{+0.5}_{-1.3}$	Bulge	(1), (2), (3)
XTE J0929-314	43.6	5.40	2.7×10^{-10}	$<9.7^{+25}_{-7.7} \times 10^{-12}$	0.01	He,C,O	8^{+7}_{-3}	Field	(1), (2), (3), (4)
MAXI J0911-655	44.3	2.94	1.37×10^{-10}	$(0.5-3.8) \times 10^{-10}$	0.028	⋯	$10.1^{+0.112}_{-0.111}$	NGC 2808	(1), (5)
IGR J16597-3704	46.0	9.51	1.97×10^{-10}	5.5×10^{-10}	0.01	⋯	$7.2^{+0.299}_{-0.288}$	NGC 6256	(1), (6)
Swift J1756.9-2508	54.7	5.49	1.54×10^{-9}	$1.9^{+2.5}_{-1.7} \times 10^{-11}$	0.015	He	8^{+4}_{-4}	Bulge	(1), (2), (3), (4)
NGC 6440 X-2	57.3	4.86	1.58×10^{-10}	$1.3 \pm 0.7 \times 10^{-12}$	0.008	⋯	$8.2^{+0.248}_{-0.241}$	NGC 6440	(1), (2), (3)
MAXI J1957+032	60.9	3.18	4.91×10^{-10}	0.8×10^{-10}	0.085	⋯	5 ± 2	Field	(1), (7)
IGR J17494-3030	75.0	2.66	9.35×10^{-11}	2.6×10^{-12}	0.02	⋯	8?	Field	(1), (8)
Persistent sources									
RX J0042.3+4115	7.7	?	1.36×10^{-12}	⋯	0.088	⋯	785	M31	(9)
4U 1728-34	10.8?	⋯	2.08×10^{-9}	$2.6 \pm 1.6 \times 10^{-9}$	⋯	⋯	3.3 ± 0.5	Bulge	(1), (2)
4U 1820-303	11.4	⋯	5.02×10^{-9}	$1.2 \pm 0.8 \times 10^{-8}$	0.07	He	8.0 ± 0.108	NGC 6624	(1), (2), (3), (4)
4U 0513-40	17.0	⋯	1.33×10^{-10}	$1.2 \pm 0.6 \times 10^{-9}$	0.05	He	$12.0^{+0.134}_{-0.133}$	NGC 1851	(1), (2), (3), (4)
2S 0918-549	17.4	⋯	1.12×10^{-10}	$2.6 \pm 1.5 \times 10^{-10}$	⋯	He,C,O?	3.0 ± 0.2	Field	(1), (2), (4)
4U 1543-624	18.2	⋯	7.27×10^{-10}	$1.3^{+1.8}_{-1.2} \times 10^{-9}$	0.03	C,O	9.2 ± 2.3	Field	(1), (2), (3), (4)
4U 1850-087	20.6	⋯	1.04×10^{-10}	$2.8 \pm 1.4 \times 10^{-10}$	0.04	Ne-excess	$7.4^{+0.240}_{-0.233}$	NGC 6712	(1), (2), (3), (4)
M15 X-2	22.6	⋯	6.71×10^{-11}	$3.8 \pm 1.9 \times 10^{-10}$	0.03	He?,C?	10.7 ± 0.095	NGC 7078	(1), (2), (3), (4)
47 Tuc X9	28.2	?	4.73×10^{-12}	$(0.3 - 1) \times 10^{-11}$	0.015	C,O	4.5 ± 0.031	NGC 104	(1), (10)
IGR J17062-6143	38.0	6.11	5.53×10^{-11}	$1.8^{+1.8}_{-0.5} \times 10^{-10}$	0.01	O	7.3 ± 0.5	Field	(1), (3), (11)
4U 1626–67	41.5	7680	2.69×10^{-10}	$8^{+14}_{-6} \times 10^{-10}$	0.04	C,O,Ne	8	Field	(1), (2), (3), (4)
4U 1916-053	50.0	⋯	5.57×10^{-10}	$6.3 \pm 3.7 \times 10^{-10}$	0.012	He,N	5.8 ± 0.3	Field	(1), (2), (3), (4)
4U 0614+091	51.3	⋯	1.77×10^{-9}	$3.9 \pm 2.3 \times 10^{-10}$	0.014	C,O	2.0 ± 0.02	Field	(1), (2), (3), (4)

Notes. The sample is divided into transients (top) and persistent sources (bottom).
References: (1) Armas Padilla et al. (2023); (2) Heinke et al. (2013); (3) Avakyan et al. (2023); (4) van Haaften et al. (2012c); (5) Sanna et al. (2017); (6. Sanna et al. (2018); (7) Sanna et al. (2022); (8. Ng et al. (2021); (9) Ma et al. (2026); (10) Tudor et al. (2018); (11) Hernández Santisteban et al. (2019).

combination of compact mass-accretors, ultra-short orbits and mass-donors with different chemical compositions (see Nelemans & Jonker 2010). (4) It has been proposed that UCXBs are possible progenitor candidates of MSPs (see, e.g., Alpar et al. 1982; Yang et al. 2023; Guo et al. 2025). (5) UCXBs provide important constraints on the binary evolution theory under extreme conditions, e.g., the common-envelope (CE) evolution, the angular-momentum loss mechanisms, the accretion physics of compact objects, etc. (see Tauris & van den Heuvel 2023).

The observations of UCXBs can be traced back to the 1970s, and the number of UCXB candidates increased significantly as more X-ray satellites were launched after the 1990s, such as the ROSAT observatory, the Chandra X-ray Observatory, the XMM-Newton mission, the Rossi X-ray Timing Explorer (RXTE), etc. (see Armas Padilla et al. 2023). Up to now, there are about 50 UCXB candidates, in which 49 sources have been discovered in the Galaxy and one is in M31 (see Armas Padilla et al. 2023; Moutard et al. 2024; Zhang et al. 2024a; Ma et al. 2026). In the Galaxy, half of UCXB candidates are located in the bulge, and ∼90% of sources are located within 10 kpc of the Sun (see Armas Padilla et al. 2023). Armas Padilla et al. (2023) suggested that there are at least two distinct classes for UCXB candidates, as follows: (1) Persistent systems with orbital periods <30 minutes account for the UCXB population in globular clusters. (2) Transients (70%) with orbital periods between 40 and 60 minutes are dominated by sources formed in the Galactic field.

In Table 1, we list the observational properties of 22 confirmed UCXBs that have been identified with high confidence based on their precise measurements for orbital periods, including nine transients and 13 persistent sources (see, e.g., in't Zand et al. 2007; Cartwright et al. 2013; Heinke et al. 2013; Armas Padilla et al. 2023; Ma et al. 2026). In the Galaxy, there are 21 confirmed UCXBs, in which nine in the field, eight in globular clusters and four in the bulge. So far, more than half of the observed UCXBs have been discovered in globular clusters or in the bulge. Meanwhile, about half of

the confirmed UCXBs are the accreting MSPs (see Armas Padilla et al. 2023).

In the observations, most of the currently confirmed UCXBs have been suggested to contain NS accretors though they are not identified exclusively (see, e.g., Sazonov et al. 2020; Coti Zelati et al. 2021). It is worth noting that three BH-UCXB candidates have been suggested, i.e., 47 Tuc X9 (see Bahramian et al. 2017; Tudor et al. 2018), RZ 2109 (see Steele et al. 2014; Dage et al. 2024) and RX J0042.3+4115 (i.e., M31 UCXB-1; see Ma et al. 2026). For more discussions on BH-UCXBs, see Section 6.

Due to the ultra-short orbits, the mass-donors in UCXBs could be constrained to be hydrogen-poor, fully or partially degenerate stars (e.g., WDs or He stars; see Rappaport et al. 1982; Nelson et al. 1986; Deloye & Bildsten 2003). According to the spectra in some UCXBs, it has been suggested that the accreted material onto NSs is composed of He or C and O, which can be used to identify the mass-donors in UCXBs (see Nelemans et al. 2004, 2006; van Haaften et al. 2012c). In addition, Galloway et al. (2008) suggested that thermonuclear (type I) X-ray bursts from accreting NSs have distinct properties independent of the accreted material, which may help to constrain the compositions of the mass-donors in UCXBs (see also Cumming 2003).

In dense star clusters (e.g., globular clusters), UCXBs are believed to result from dynamical interactions (tidal captures or stellar encounters) with a high probability (see, e.g., Verbunt 1987; Bailyn & Grindlay 1987; Davies et al. 1992; Davies & Hansen 1998; Ivanova et al. 2005; Verbunt 2005; Voss & Gilfanov 2007). In the Galactic field, however, their formation is dominated by isolated binary evolution. It has been proposed that the mass-donors in UCXBs could be a WD (the WD donor channel), a He star (the He star donor channel) or an evolved main-sequence (MS) star (the evolved MS donor channel; for a review see Nelemans & Jonker 2010). Meanwhile, a UCXB can also be formed through the accretion-induced collapse (AIC) of WDs in binaries, known as the AIC channel (see Liu & Wang 2023).

In this review, we mainly focus on the formation and evolution of UCXBs. In Sections 2–5, we review the WD donor channel, the He star donor channel, the evolved MS donor channel and the AIC channel, respectively. In Section 6, we discuss the observed BH-UCXB candidates and the formation channels to BH-UCXBs. In Section 7, we make a comparison between theoretical results and observations. The impacts of UCXBs on some research fields are discussed in Section 8. A summary and perspective are provided in Section 9.

2. The WD Donor Channel

2.1. Formation and Evolution of NS+He WD Systems

In this channel, an NS accretes He-rich material from a He WD through RLOF, in which the mass-transfer is driven by GW radiation (see, e.g., Pringle & Webbink 1975; Iben et al. 1995; Belczynski & Taam 2004; van Haaften et al. 2012b; Yu et al. 2021; Chen et al. 2022b). There is one evolutionary scenario to form NS+He WD systems and then produce UCXBs (see Figure 1). In the primordial binary, the primary star evolves faster onto the giant branch stage and begins transferring material onto its companion. Due to the large mass-ratio, the mass-transfer process becomes dynamically unstable, leading the binary into a CE stage. During this stage, the companion star orbits the core of the primary, and their orbital energy is converted into the internal energy of the envelope. If sufficient orbital energy is available, the CE can be ejected, resulting in the formation of a He star+MS binary. The He star then evolves and collapses into an NS via a supernova (SN) explosion. If the system survives, an NS+MS binary is formed. Subsequently, magnetic braking (MB) causes the donor star to fill its Roche lobe near the end of the MS or during the Hertzsprung gap (HG) phase, initiating mass-transfer onto the NS. Once this mass-transfer concludes, an MSP+He WD binary is produced. At this stage, the He WD is extremely low-mass and the orbital period is relatively short. GW radiation then causes the orbit to shrink until the He WD fills its Roche lobe. The system subsequently evolves into a UCXB, eventually forming an isolated MSP or a pulsar +planet-like system. For more studies on the formation and evolution of NS+WD systems, see, e.g., Lü et al. (2017), Toonen et al. (2018), Gu et al. (2020), Li & Chen (2024), Yang & Chen (2025), Li et al. (2025b), Kang et al. (2026), etc.

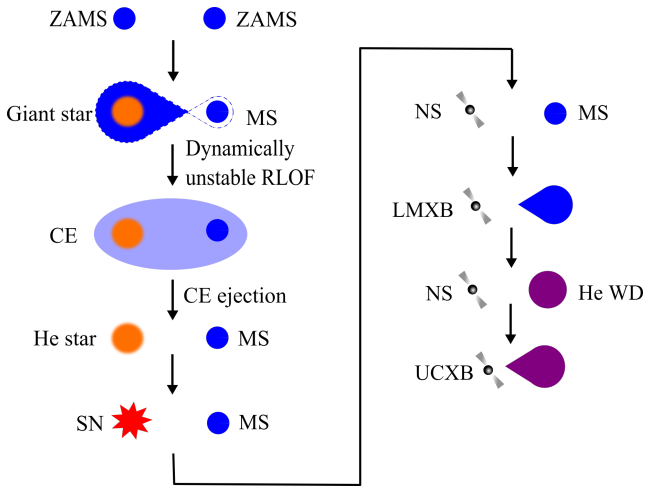


Figure 1. Formation of NS+He WD systems that can evolve into UCXBs.

2.2. Parameter Space for UCXBs

By modeling the formation of UCXBs with the standard MB prescription from Rappaport et al. (1983), previous studies argued that the parameter space from the WD donor channel is relatively small (see van der Sluys et al. 2005a, 2005b). Meanwhile, it has been suggested that it is impossible to produce UCXBs if a weaker MB is adopted (see van der Sluys

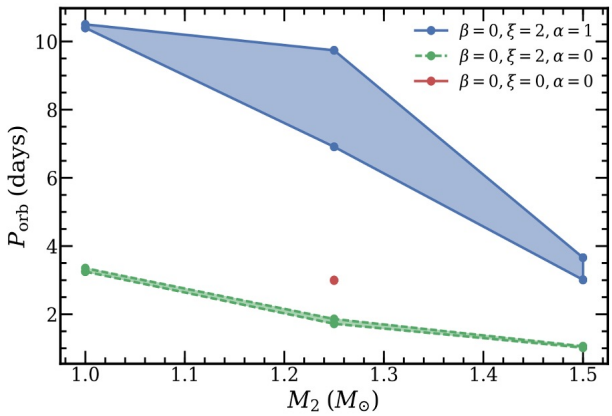


Figure 2. Parameter space for producing UCXBs through the WD donor channel, in which the initial NS mass is assumed to be 1.3 $M_\odot$. It has been suggested that models with $\beta = 0$, $\xi = 2$ and $\alpha = 1$ can better reproduce the properties of the observed X-ray binaries (see Van et al. 2019). Source: From Chen et al. (2021).

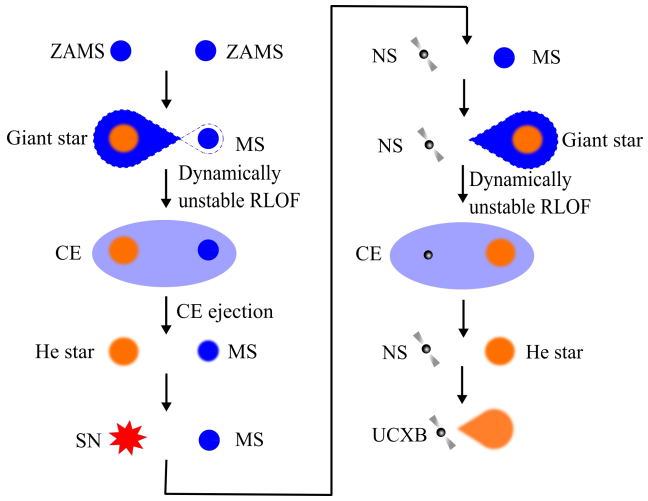


Figure 3. Formation of NS+He star systems that can evolve into UCXBs.

et al. 2005a, 2005b). In addition, Istrate et al. (2014) suggested that the parameter space of MSPs with extremely low-mass WD companions is also very small if the standard MB prescription is adopted.

By using a newly suggested MB prescription from Van et al. (2019), Chen et al. (2021) recently found that the initial orbital period range of LMXBs forming UCXBs becomes significantly wider (see Figure 2; see also Deng et al. 2021). These studies suggested that a stronger MB is needed for modeling the formation of UCXBs. Yang & Chen (2025) arrived at a similar conclusion by modeling the formation of MSP+He WDs with a different MB prescription.

The stability of mass-transfer from a WD onto an NS is still being debated. In earlier studies, a critical WD mass is used to determine the stability of mass-transfer, in which the critical mass ranges from 0.35 to 1.25 $M_\odot$. In most of these studies, a semi-analytic method is adopted to model the evolution of NS +WD binaries (see, e.g., Verbunt & Rappaport 1988; Paschalidis et al. 2009; Yungelson et al. 2002; van Haaften et al. 2012b; Yu et al. 2021). According to the results of hydrodynamic simulations, Bobrick et al. (2017) argued that only binaries including He WDs with masses $<0.2\,M_\odot$ can undergo stable mass-transfer and then produce UCXBs. In addition, by considering the detailed structure of He WDs, Chen et al. (2022b) modeled the evolution of NS+He WD binaries with detailed binary evolution computations, suggesting that the critical WD mass is 0.45 $M_\odot$. The main reason for the difference between the two studies is that Bobrick et al. (2017) included the effect of disk wind, which causes extra angular momentum loss and thereby leads to a smaller critical mass. Previous studies indicate that it is hard to produce UCXBs with CO WD donors (see, e.g., Bobrick et al. 2017; Chen et al. 2022b). Moreover, Sengar et al. (2017) suggested that the WD donor channel can well explain the observed properties of UCXBs with high He abundances.

These UCXBs, along with detached NS+He WD binaries that have short orbital periods, can generate strong GW emission in the mHz band, detectable by LISA, TianQin and Taiji. However, the number of detectable sources remains highly uncertain. He et al. (2024) modeled the Galactic population of NS+CO/ONe WD systems, predicting that approximately tens to hundreds of such systems could be detected by LISA. In a complementary estimate, Tauris (2018) suggested that LISA could detect at least 100 UCXBs with NS accretors.

Additionally, 4U 1820-303 is one of the most compact binaries, which has a negative orbital-period derivative in globular cluster NGC 6624 (see, e.g., Sansom et al. 1989; Chou & Grindlay 2001; Peuten et al. 2014). According to the WD donor channel, Jiang et al. (2017) used an evolutionary circumbinary disk assumption to account for the negative orbital-period derivative of this source. However, Chou & Grindlay (2001) argued that 4U 1820-303 may originate from a hierarchical triple system with a ∼1.1 day period companion based on its stable long-term modulation.

3. The He Star Donor Channel

3.1. Formation and Evolution of NS+He Star Systems

In this channel, an NS accretes matter from a He star through RLOF, in which the He star fills its Roche-lobe due to the rapid orbital shrinkage induced by GW radiation (see, e.g., Savonije et al. 1986; Heinke et al. 2013; Wang et al. 2021). There is one evolutionary scenario to form NS+He star systems and then produce UCXBs (see Figure 3). The primordial primary first fills its Roche lobe during its subgiant phase, initiating a dynamically unstable mass-transfer because of its large mass-ratio. In this case, a CE would be formed. If

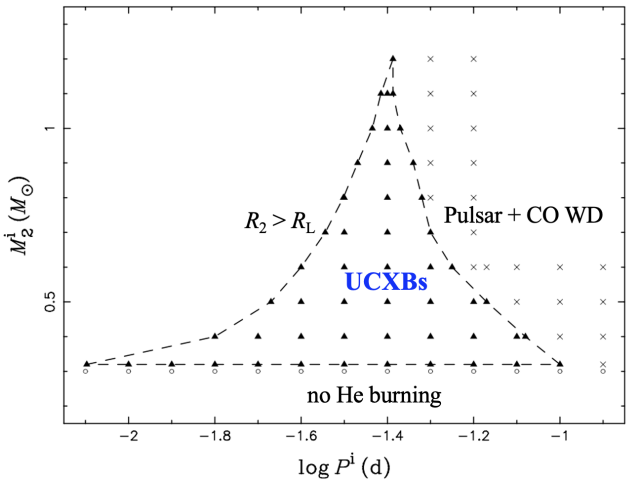


Figure 4. Parameter space for producing UCXBs through the He star donor channel, in which the initial NS mass is assumed to be 1.4 $M_\odot$. The filled triangles are for those resulting in the formation of UCXBs. Open circles are those for which the masses of He star donors are too low to ignite He in their center. Crosses indicate systems that will experience high mass-transfer rates when the He star donors evolve into the subgiant stage, leading to the formation of intermediate-mass binary pulsars. Source: From Wang et al. (2021).

the CE can be ejected, the primordial primary will evolve into a He star. The He star continues to evolve and will explode as an SN, leading to the formation of an NS. Subsequently, the primordial secondary fills its Roche-lobe when it evolves to the giant stage, leading to the formation of the second CE. After the ejection of the CE, an NS+He star system would be produced. The He star will fill its Roche-lobe due to the contraction of the orbit resulting from the GW radiation. In this case, the mass-transfer is stable and the system evolves into a UCXB (see Wang et al. 2021). For more studies on the formation and evolution of NS+He star systems, see, e.g., Guo et al. (2023), Li et al. (2024), Guo et al. (2024a), Yang et al. (2025b), Deng et al. (2025), Benvenuto & Horvath (2026), etc.

3.2. Parameter Space for UCXBs

By computing the evolution of an NS+He star system with a tight orbit, Savonije et al. (1986) first confirmed that NSs can be accompanied by He stars with low masses. It has been suggested that 50%−80% of UCXBs might be produced through the He star donor channel (see Zhu et al. 2012). Wang et al. (2021) recently followed the long-term evolution of NS+He star systems, thereby obtaining the initial parameter space for the formation of UCXBs (see Figure 4). The parameter space in Figure 4 is set by the following criteria: (1) The lower boundary of the contour is determined by the condition that the masses of He stars should be larger than 0.32 $M_\odot$, below which He burning would be extinguished in their center (see also Han et al. 2002). (2) The left boundary is constrained by the requirement that the He star fills its Roche-lobe during the zero-age MS phase. (3) The systems beyond the right boundary undergo high mass-transfer rates when the He stars evolve into the subgiant stage, forming intermediate-mass binary pulsars.

Wang et al. (2021) found that all NS+He star systems forming UCXBs can be detectable by LISA within a distance of 15 kpc. These NS+He star systems are even be visible as LISA sources within a distance of 100 kpc. The average timescale that the NS +He star binary appears as a LISA source is about 33 Myr within a distance of 15 kpc. By using a detailed binary population synthesis method (see Han et al. 2020), Wang et al. (2021) estimated that the Galactic rates of UCXB-LISA sources are $\sim$3.1−11.9 Myr^{-1}, and that the number of UCXB-LISA sources can be $\sim$1−26 through the calibration of UCXB observations in the Galaxy.

3.3. Black Widows With Extremely Low Masses

Black widows (BWs) are a subclass of eclipsing MSPs in compact binaries with low-mass companions (see, e.g., Chen et al. 2013; Roberts 2013; Benvenuto et al. 2014). Their companions are generally thought to be gradually stripped by irradiation-driven winds powered by γ-ray emission and relativistic particles from the MSP, a mechanism commonly referred to as the evaporation process (e.g., Kluzniak et al. 1988; Ruderman et al. 1989). BWs provide valuable laboratories for investigating the evolutionary pathways of close NS binaries, including the magnetic-field decay, the angular-momentum loss, accretion efficiency, constraints on the NS equation of state, etc. (e.g., Cumming et al. 2001; Tauris et al. 2012; Van et al. 2019).

With the growing number of BW systems identified, it has become increasingly evident that BWs can be divided into two subpopulations based on their companion masses (M_2). Figure 5 shows the distribution of BWs in the $P_{\rm orb} - M_2$ plane. Systems located in region (A) correspond to BWs with M_2 in the range of 0.01−0.05 $M_\odot$, while those in region (B) have extremely low-mass companions with $M_2 \lesssim 0.01\,M_\odot$ (see Guo et al. 2022). The origin of BWs in region (B) cannot be explained by conventional evolutionary scenarios that fail to reduce the companion mass to such small values within the Hubble time (see, e.g., Chen et al. 2013; Ginzburg & Quataert 2020).

Based on the He star donor channel for the formation of UCXBs (see Wang et al. 2021), Guo et al. (2022) considered the evaporation process into the subsequent evolution. Their models successfully reproduce the observed properties of BWs with extremely low-mass companions ($M_2 \lesssim 0.01\,M_\odot$), including PSRs J1719-1438, J2322-2650, J1653-0158, etc. More recently, the Five-hundred-meter Aperture Spherical radio Telescope (FAST) discovered a binary pulsar PSR J1953+1844 (i.e., M71E) in a 53 minute orbit, which is currently the shortest orbital-period binary pulsar known (see, e.g., Han et al. 2021; Pan et al. 2023). This system can also be naturally explained through the UCXBs with the He star donor channel (e.g., Yang et al. 2023; Guo et al. 2024b). In addition, Vleeschower et al. (2024)

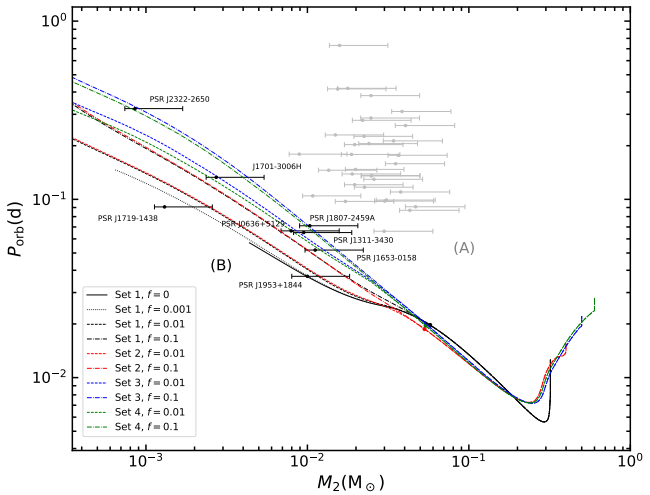


Figure 5. The evolutionary tracks of NS+He star binaries with different initial He star masses (M_2) and evaporation efficiencies (f), along which the systems may evolve through the UCXB phase. Different colors represent the NS+He star systems with different initial parameters, hereafter referred to as sets 1–4 (see also Guo et al. 2022). Set 1 starts with $M_2^{\rm i} = 0.32\,M_\odot$ and $\log(P_{\rm orb}^{\rm i}/{\rm day}) = -1.90$, while sets 2–4 correspond to progressively higher initial He star masses ($M_2^{\rm i} = 0.40$, 0.50, and $0.60\,M_\odot$) and wider initial orbits ($\log(P_{\rm orb}^{\rm i}/{\rm day}) = -1.80$, -1.65, and -1.55). Colored dots mark the onset of the evaporation process for each set. Black symbols in region (B) indicate BWs with $M_2 < 0.01\,M_\odot$, while gray symbols in region (A) represent BWs with M_2 in the range 0.01–$0.05\,M_\odot$. Observational data for BWs are taken from the ATNF Pulsar Catalogue: http://www.atnf.csiro.au/research/pulsar/psrcat (version 1.70, 2023 May; Manchester et al. 2005). The error bars indicate the minimum and maximum companion masses, corresponding to orbital inclination angles of 90° and 26° (the 90% probability limit), respectively. Compared with Figure 4 in Guo et al. (2022), we added a new BW in this figure, i.e., PSR J1953+1844.

recently reported the discovery of the MSP J1701-3006H (i.e., M62H) in the globular cluster M62 using MeerKAT, hosting an extremely low-mass companion with a median mass of $\sim 0.0027\,M_\odot$ and an orbital period of 2.7 hr. Such a low companion mass for M62H indicates an evolutionary origin through the He star donor channel (see Figure 5).

BWs have long been proposed as a possible evolutionary channel leading to isolated MSPs (e.g., Kluzniak et al. 1988; van den Heuvel & van Paradijs 1988). However, the standard channel fails to account for the observed isolated MSP population within the Hubble time (e.g., van Haaften et al. 2012a; Ginzburg & Quataert 2020). The simulations by Guo et al. (2022) indicate that the companion mass can be reduced to $<10^{-3}\,M_\odot$, or even $<10^{-5}\,M_\odot$. Therefore, the BWs formed through the He star donor channel are promising progenitors for isolated MSPs.

4. The Evolved MS Donor Channel

4.1. Formation and Evolution of NS+MS Systems

In this channel, an NS accretes matter from an evolved MS donor with initial orbital periods below the bifurcation period, eventually evolving into UCXBs (see Podsiadlowski et al. 2002; Chen et al. 2020; Chen & Liu 2025). In the classic scenario, LMXBs with initial orbital periods above the bifurcation period will produce diverging systems, otherwise forming converging systems (see, e.g., Pylyser & Savonije 1988, 1989). The evolutionary scenario for this channel is similar to that of the WD donor channel (see Figure 1), but the formed NS+MS systems with initial orbital periods should be below the bifurcation period.

Previous studies indicate that the bifurcation period is sensitive to the mechanisms of angular-momentum loss, especially for the prescriptions of the MB laws (see, e.g., Ergma 1996; Podsiadlowski et al. 2002; van der Sluys et al. 2005a, 2005b; Ma & Li 2009b; Shao & Li 2015; Chen et al. 2020, 2021; Deng et al. 2021). Some NS+MS binaries can evolve into detached MSP+WD systems if their initial orbital periods are very close to the bifurcation periods (see Chen et al. 2020). Subsequent evolution overlaps with the WD donor channel. In the standard MB case, it requires fine-tuning initial orbital periods to form MSP+WD systems with short orbital periods (WDs can fill their Roche lobes due to GW radiation in the Hubble time) for those NS+MS binaries (see Istrate et al. 2014). Otherwise, NS+MS systems always experience a mass-transfer rather than a detached stage even if their initial orbital periods are shorter than the bifurcation periods (see Chen et al. 2020). Some efficient MB mechanisms can alleviate the fine-tuning problem and widen the range of initial orbital periods that can form detached MSP+WD systems (see, e.g., Chen et al. 2021; Yang & Chen 2025).

For intermediate-mass X-ray binaries (IMXBs, donor-star masses $\geqslant 2\,M_\odot$), the mass-transfer occurs on a short thermal timescale because the material is transferred from the more massive donor star to the less massive NS. In principle, IMXBs spend most of their X-ray active lifetime as LMXBs. Therefore, some IMXBs can first evolve into LMXBs and then evolve toward UCXBs (see, e.g., Li 2002; Podsiadlowski et al. 2002; Xu & Li 2007; Lin et al. 2011; Shao & Li 2012; Li 2020). Because intermediate-mass stars without convective envelopes are not generally expected to experience the MB process, it seems difficult for IMXBs to evolve into UCXBs. However, previous studies indicate that some pre-IMXBs with initial orbital periods very close to the bifurcation periods can still evolve into UCXBs due to the MB process once donor stars develop convective envelope (i.e., donor-star masses $\leqslant 1.5\,M_\odot$; see, e.g., Istrate et al. 2014; Chen et al. 2020). About 5% of intermediate-mass stars (so-called Ap/Bp stars) possess anomalously strong magnetic fields, which can drive IMXBs to evolve toward UCXBs by an anomalous MB mechanism induced by the coupling between the irradiation-driven wind and the magnetic field (see Chen & Podsiadlowski 2016). Furthermore, the tidal torque between an IMXB and a surrounding circumbinary disk can also efficiently extract

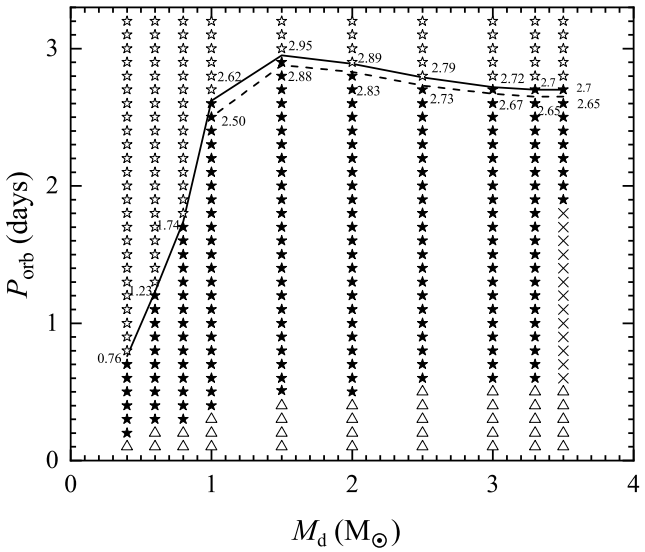


Figure 6. Parameter space of the pre-LMXBs/IMXBs for producing UCXBs, in which the initial NS mass is assumed to be 1.4 $M_\odot$. The solid stars show the pre-LMXBs/IMXBs that can evolve into UCXB-LISA sources within a distance of 1 kpc. The solid curve denotes the bifurcation periods of LMXBs/IMXBs with different initial masses of donors, whereas the dashed curve presents the minimum initial orbital period for the progenitors of UCXB-LISA sources within a distance of 10 kpc. The open stars, the open triangles and the crosses indicate the systems that will not produce UCXBs. Source: From Chen et al. (2020).

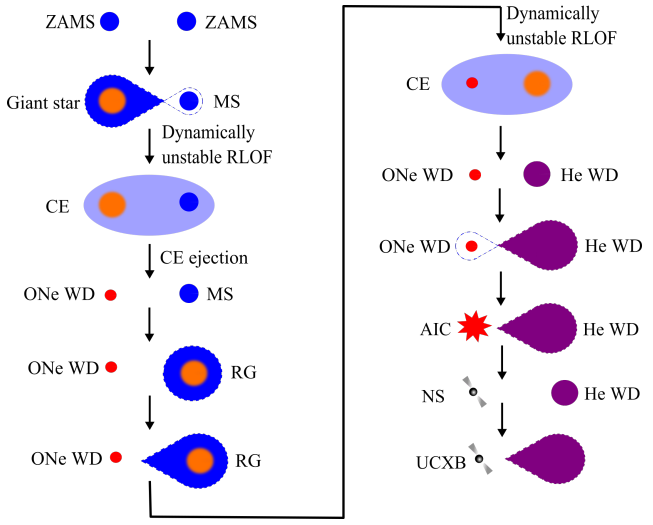


Figure 7. Formation of ONe WD+He WD systems that undergo the AIC process and evolve into UCXBs finally.

angular momentum from the system and induce the formation of an UCXB (see Ma & Li 2009a).

4.2. Parameter Space for UCXBs

Adopting the standard MB prescription given by Rappaport et al. (1983), Chen et al. (2020) used the stellar evolution code MESA to simulate the evolution of a large number of pre-LMXBs/IMXBs containing NS+MS systems. Their results show that UCXBs could be formed by NS+MS systems with a 0.4−3.5 $M_\odot$ MS companion and an initial orbital period shorter than the bifurcation periods (see Figure 6). As shown in Figure 6, most pre-LMXBs/IMXBs with initial orbital periods less than the bifurcation periods can evolve into UCXB-LISA sources within a distance of 1 kpc, but the parameter space is in a very narrow range within a distance of 10 kpc. According to the calculated parameter space, Chen et al. (2020) estimated that the Galactic rates of UCXB-LISA sources are $\sim$2−2.6 Myr^{-1} based on binary population synthesis simulations. They obtained the number of UCXB-LISA sources in the range of 240–320 by considering the contribution of UCXBs in globular clusters.

5. The AIC Channel

5.1. Formation and Evolution of AIC Systems

In this channel, an ONe WD accretes matter from a He WD, eventually collapsing into an NS when the ONe WD increases its mass close to the Chandrasekhar limit ($M_{\rm Ch}$; see Nomoto et al. 1979; Taam & van den Heuvel 1986; Nomoto & Kondo 1991; Brooks et al. 2017b). After that, the NS continues to accrete matter from the He WD, forming a UCXB finally (see Liu & Wang 2023). This channel is related to the AIC process of ONe WDs in binaries (for a recent review see Wang & Liu 2020). AIC events are a type of faint optical transient and exhibit rapid changes in brightness, which are important for producing isolated NSs and NS systems (see, e.g., Woosley & Baron 1992; Fryer et al. 1999; Dessart et al. 2007). To date, there is no direct detection for the existence of AIC events though there exists a lot of indirect evidence in observations (see, e.g., Canal et al. 1990; Ivanova et al. 2008; Boyles et al. 2011; Tauris et al. 2013; Ablimit 2019; Ruiter et al. 2019; Wang et al. 2026). For more studies on the formation and evolution of AIC systems, see, e.g., Chen et al. (2011), Brooks et al. (2017a), Wang et al. (2017), Wang (2018), Liu et al. (2018), Wu et al. (2019); Liu & Wang (2020), Wang et al. (2022), Wu et al. (2023a, 2023b), Zhang et al. (2024b), Ruiter & Seitenzahl (2025), Batziou et al. (2025), Meng (2025), etc.

There is one evolutionary scenario to form ONe WD+He WD systems, eventually producing UCXBs through the AIC process (see Figure 7). The primordial primary first fills its Roche lobe during the giant phase, leading to a dynamically unstable mass-transfer process. In this case, a CE is supposed to be formed. If the CE can be ejected, an ONe WD+MS system would be produced. Subsequently, the primordial secondary continues to evolve, and will fill its Roche-lobe at the red-giant stage. During this phase, the mass-transfer is also dynamically unstable and a second CE may be formed. After the second CE ejection, the primordial secondary will evolve into a He WD. After that, the He WD will fill its Roche-lobe due to the orbital shrinks driven by the GW radiation. The

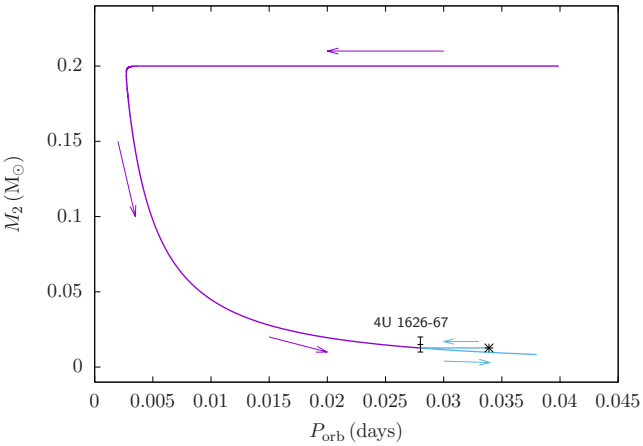


Figure 8. An alternative evolutionary track for the formation and evolution of 4U 1626–67. The purple line shows the evolutionary track before the AIC process, whereas the blue line presents the evolutionary track after the AIC process. The asterisk represents the start of the position just after the AIC process. Source: From Liu & Wang (2023).

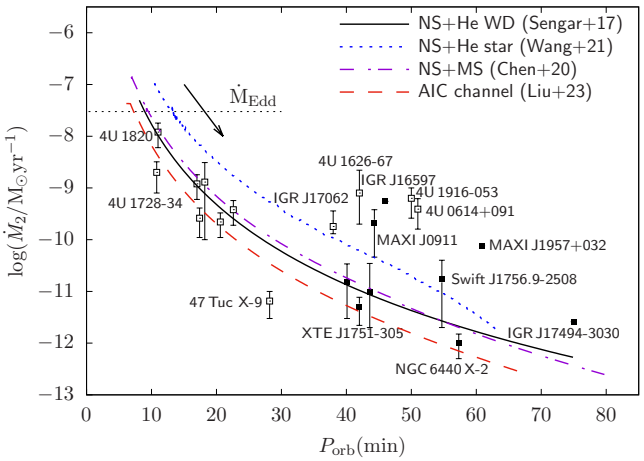


Figure 9. Comparison between the theoretical evolutionary tracks from different channels and the observational data in the mass-transfer rate versus the orbital period diagram. The black solid line shows the numerical relation fit based on the WD donor channel (see Sengar et al. 2017), the blue dotted line is based on the He star donor channel (see Wang et al. 2021), the purple dot-dotted line is based on the evolved MS donor channel (see Chen et al. 2020) and the red dashed line is based on the AIC channel (see Liu & Wang 2023). The open squares and solid squares denote persistent sources and transient sources in Table 1, respectively. Note that it is still controversial for the orbital periods of 4U 1728-34 (see Heinke et al. 2013). The black dotted line is $\dot{M}_{\rm Edd}$ for an NS accreting He-rich matter.

accreted He-rich matter burns stably on the surface of the ONe WD, leading to the mass-growth of the WD. When the ONe WD mass increases to $M_{\rm Ch}$, an AIC event is supposed to occur, leading to the formation of an NS. After that, the He WD may fill its Roche-lobe again owing to GW radiation, leading to the formation of a UCXB (see Liu & Wang 2023).

5.2. UCXBs From the AIC Channel

4U 1626–67 is a type of peculiar UCXB, containing a newly formed NS and an ultra-light companion. However, the evolutionary path for 4U 1626–67 is still under hot debate. It has been suggested that peculiar newly formed NS+ultra-light companion systems like 4U 1626–67 could represent evidence for the existence of AIC events (see Tauris et al. 2013). Liu & Wang (2023) carried out a series of ONe WD+He WD systems for producing AIC events, suggesting that the NS binaries would evolve to UCXBs when the He WDs refill their Roche lobes. They found that the properties of 4U 1626–67 can be reproduced by the AIC channel. Figure 8 shows a possible evolutionary track for the formation and evolution of 4U 1626–67 based on the AIC channel. As shown in this figure, the He WD would refill its Roche-lobe after the AIC process, resulting in the production of a UCXB with a newly formed NS and an ultra-light He WD. The observed orbital period and companion mass in 4U 1626–67 can be well reproduced by the AIC channel, although there are still some uncertainties regarding its origin, especially for the high mass-transfer rate (for more discussions see Liu & Wang 2023).

In addition, UCXB XTE J1751-305 is a transient accreting MSP with an orbital period of 42 min (Markwardt et al. 2002). It has been proposed that XTE J1751−305 may also originate from the AIC channel (see Liu & Wang 2023). The asteroseismology models indicate that the accreting matter onto the NS in XTE J1751-305 is composed mostly of He (see Lee 2014; Strohmayer & Mahmoodifar 2014). Meanwhile, the observed parameters in XTE J1751−305 can be only covered by the AIC channel for UCXBs in the mass-transfer rate versus the orbital period diagram (see Figure 9).

6. BH-UCXBs

6.1. The Observed BH-UCXB Candidates

It has been suggested that the mass-accretors in three UCXBs may be BHs, as follows: (1) 47 Tuc X9 is an LMXB in the globular cluster 47 Tucanae. Miller-Jones et al. (2015) first identified a radio counterpart to 47 Tuc X9, suggesting that the ratio of radio/X-ray luminosity for 47 Tuc X9 is more consistent with BH-LMXBs and that the mass-donor might be a WD. Bahramian et al. (2017) recently reported the orbital period of 47 Tuc X9 as $28.18^{+0.02}_{-0.02}$ minutes based on the Chandra data. They confirmed that this system is a BH-UCXB candidate in the Galaxy, suggesting that the mass-donor may be a CO WD. In a further work, Tudor et al. (2018) speculated that a BH+He star system could evolve into 47 Tuc X9. (2) RZ 2109 is a globular cluster ultraluminous X-ray source in the elliptical galaxy NGC 4472. It has been suggested that RZ 2109 is a BH-UCXB candidate with a WD donor (see Steele et al. 2014; Dage et al. 2024). (3) M31 UCXB-1 is one of the brightest X-ray sources in the bulge of M31. Zhang et al. (2024a) reported an orbital period of about 465 s from this

source based on XMM-Newton and Chandra data. Ma et al. (2026) suggested that M31 UCXB-1 is a BH+WD system with the shortest orbital period among the known UCXBs.

6.2. Formation Channels

The formation path to BH-UCXBs is still highly uncertain. In globular clusters, dynamical interactions that pair BHs with companion stars are probably the main formation channel for BH-UCXBs (see, e.g., Ivanova et al. 2005; Xuan et al. 2025). While in the Galactic field, similar to the formation of NS-UCXBs, there are also three classic formation channels, as follows: (1) The WD donor channel. According to detailed stellar evolution models with the convection- and rotation-boosted MB prescription, Yang et al. (2025a) confirmed that isolated BH+MS binaries can evolve into BH-UCXBs with orbital periods of 7.7 minutes as in M31 UCXB-1, in which a low-mass WD transfers matter onto a BH. Motivated by the fact that most massive stars are born in triple systems, Xuan et al. (2025) argued that wide BH+WD systems can naturally form UCXBs via the eccentric Kozai–Lidov mechanism (see Lidov 1962; Kozai 1962). (2) The He star donor channel. Qin et al. (2024) recently studied the formation and evolution of BH-UCXBs via the He star donor channel in a systematic way. Their simulations indicate that some newly formed BH+He star binaries after the CE stage could form UCXB-LISA sources with a maximum GW frequency $\sim$5 mHz, which can be detected by LISA even at a distance of 100 kpc. (3) The evolved MS donor channel. Qin et al. (2023) suggested that BH+MS binaries with initial orbital periods less than the bifurcation period could evolve into BH-UCXBs. They predicted that LISA will detect a few BH-UCXB GW sources based on this channel.

For the formation of BH-LMXBs (the progenitors of BH-UCXBs), however, the progenitors of the BHs should be more massive. It is proven that the removal of the massive envelope of the BH progenitors via CE evolution is very difficult in progenitor systems with low-mass ($1-2\,M_{\odot}$) donor stars due to the large binding energy of the massive envelope (see, e.g., Portegies Zwart et al. 1997; Kalogera 1999; Podsiadlowski et al. 2003b; Kruckow et al. 2016). Deng & Li (2024) argued that this difficulty can be circumvented if the BHs are formed through failed SNe, which allow BHs to be produced by stars with initial masses as low as $\sim 17\,M_{\odot}$ (see Horiuchi et al. 2014), thus avoiding the necessity of an overly massive progenitor and enabling the formation of BH-LMXBs with compact orbits (see also Wang et al. 2016).[4]

[4] The failed SN model is based on the assumption that a BH is formed depending on the compactness of the stellar core at the moment of the collapse, i.e., stellar cores with high compactness undergo failed SNe and form BHs, whereas stellar cores with low compactness produce NSs via SN explosions (see O'Connor & Ott 2011).

As alternative channels, BH-LMXBs were proposed to evolve from BH binaries with intermediate-mass ($3-5\,M_{\odot}$) donor stars by anomalous MB laws (see Justham et al. 2006) or tidal torque between the system and a surrounding circumbinary disk (see Chen & Li 2006), but the simulated effective temperatures of donor stars are significantly higher than those of the observed values. If a density spike of dark matter around the stellar-mass BH exists, Qin & Chen (2024) argued that the dynamical friction between dark matter and the mass-donors can drive the evolution of BH binaries into the observed BH-LMXBs, thus alleviating the effective temperature issue of BH-LMXBs with relatively short orbital periods.

Recently, Chen et al. (2023) proposed that NS+WD binaries can evolve into BH-UCXBs via the AIC of accreting NSs, provided the initial NS is both massive enough and able to accrete sufficient material, thus eventually collapsing into a BH. For the signatures of the NS-AIC events, it has been suggested that the magnetosphere of the NS will be disrupted and the surface of the NS would be hidden behind the event horizon of the BH during the collapse, producing strong radio signatures (possibly observable as a nonrepeating fast radio burst; see Falcke & Rezzolla 2014).

In BH-UCXBs, the WD may enter the tidal radius of the BH and trigger a tidal disruption event (TDE) if the orbital shrinkage induced by the GW radiation is stronger than the orbital expansion caused by a mass-transfer process. Yang et al. (2025a) argued that a TDE may occur after 0.12 Myr if M31 UCXB-1 is a BH-UCXB consisting of a $10\,M_{\odot}$ BH and a $0.16\,M_{\odot}$ WD.

7. Compared With Observations

7.1. The Mass-transfer Rate versus the Orbital Period Diagram

For different formation channels of UCXBs, the evolutionary tracks in the mass-transfer rate versus the orbital period diagram differ due to the distinct types or evolutionary states of their companions. Thus, UCXBs could be identified by their locations in the mass-transfer rate versus the orbital period diagram (see Figure 9). As shown in Figure 9, the majority of UCXBs can be well explained by the current existing models. Notably, some observed sources can only be accounted for by a specific formation channel (two–three sources via the He star donor channel and four–five sources via the AIC channel), offering strong evidence for their progenitors. Heinke et al. (2013) argued that the He star donor channel may explain the formation of the three wide-orbit persistent UCXBs with high mass-transfer rates. However, it is still hard for any channels to form the three wide-orbit persistent sources. It is worth noting that recent studies on different MB models have offered new possibilities (e.g., Yang & Chen 2025). Meanwhile, the upper and lower error estimates for the three wide-orbit persistent sources are not well determined (see Heinke et al. 2013).

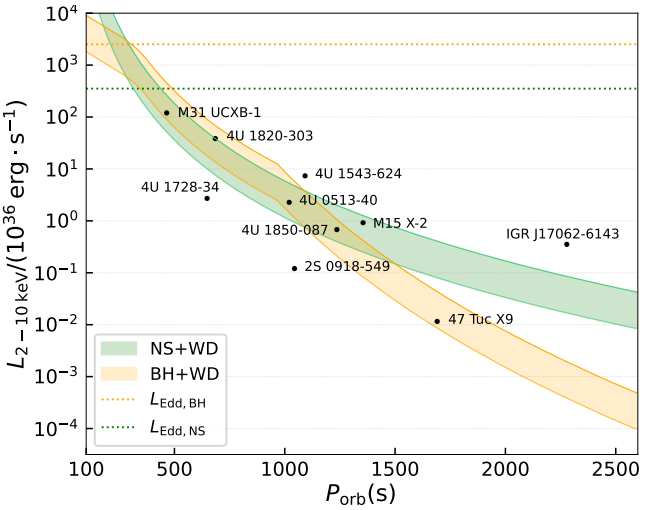


Figure 10. Numerical results of the NS/BH+WD UCXB system in the $F_{\rm X}$[2–10 keV] versus $P_{\rm orb}$ diagram. In this figure, the observed persistent UCXBs (black solid dots) in Table 1 are presented with the theoretical predictions for NS+WD (green shaded region) and BH+WD systems (orange shaded region). The theoretical results are obtained by assuming $M_{\rm NS} = 1.4\,M_\odot$ and $M_{\rm BH} = 10\,M_\odot$. Source: from Ma et al. (2026). Compared with Ma et al. (2026), we added one source in this figure, i.e., 4U 1728-34.

7.2. The X-Ray Luminosity versus the Orbital Period Diagram

Figure 10 presents the comparison between the observed persistent UCXBs and the theoretical expectations in the X-ray luminosity versus the orbital period diagram (see also Ma et al. 2026). The green and orange shaded regions denote the predicted relations for NS+WD and BH+WD binaries respectively, computed assuming an NS mass of $1.4\,M_\odot$ and a BH mass of $10\,M_\odot$. These theoretical bands are obtained from numerical models, in which the mass-transfer evolution of UCXBs is driven by the angular momentum losses due to the GW radiation (see, e.g., Nelemans & Jonker 2010; van Haaften et al. 2012c). As GW emission becomes less efficient at a wider orbit, the predicted X-ray luminosity declines toward longer periods, which is in agreement with the overall distribution of the persistent sources shown in this figure.

The numerical results indicate that, for $P_{\rm orb} \lesssim 1000$ s, the predicted 2–10 keV luminosities of NS and BH accretors are nearly identical. At longer periods ($P_{\rm orb} \gtrsim 1000$ s), however, the two evolutionary tracks separate. As the accretion rate decreases with the increasing orbital period, NSs maintain an approximately constant radiative efficiency because of their solid surfaces, whereas BHs exhibit a decline in radiative efficiency at low accretion rates (see, e.g., Narayan & Yi 1995; Watarai et al. 2001). This difference leads to a systematic divergence between the NS+WD and BH+WD predictions at longer orbital periods, enabling the two accretor types to be distinguished in this regime. Among the systems displayed in Figure 10, only 47 Tuc X9 has been proposed as a BH-UCXB candidate because of its high ratio of radio/X-ray luminosity. The location of 47 Tuc X9 in the luminosity versus period diagram is consistent with the theoretical BH+WD relation, further supporting this interpretation.

8. Impacts of UCXBs on Some Fields

UCXBs are of great significance to modern astronomical research, having important impacts on some astrophysical fields, for example, GW astronomy, multi-messenger astronomy, binary evolution, the physics of NSs under extreme conditions, etc.

8.1. GW Astronomy and Multi-messenger Astronomy

One of the most prominent impacts of UCXBs lies in GW astronomy. Current ground-based GW detectors operate primarily in the high-frequency band ($\gtrsim$10 Hz), making them sensitive to compact-object mergers such as double NSs and binary BHs shortly before coalescence (see Abbott et al. 2016, 2017). With orbital frequencies corresponding to GW frequencies of $\sim 10^{-4}$–10^{-3} Hz, UCXBs emit nearly monochromatic and long-lived GW signals that fall squarely within the sensitivity band of planned space-based detectors such as LISA, TianQin and Taiji (see, e.g., Nelemans & Jonker 2010; Tauris 2018; Chen et al. 2020, 2021). Yu et al. (2026a) studied the post-contact evolution of Roche-lobe-filling NS+WD binaries and suggested that, depending mainly on the WD mass and accretion efficiency, systems bifurcate into either stable UCXB-like mass-transfer or rapid orbital decay leading to merger. They further demonstrated that these binaries produce diverse GW signals in the LISA band, highlighting the role of the UCXB phase in producing resolvable LISA-band GW sources. Previous studies indicate that the Milky Way may host on the order of several hundred UCXBs potentially detectable by future space-based GW missions (see, e.g., Chen et al. 2020; Wang et al. 2021; Chen & Liu 2025).

Aside from their orbital GW emission in the mHz band, UCXBs hosting rapidly rotating NSs may also produce high-frequency continuous GWs arising from stellar asymmetries or r-mode oscillations, making them potential dual-band GW sources (see, e.g., Bildsten 1998; Chen 2021). In such systems, the low-frequency orbital signal and the high-frequency spin-induced component could jointly constrain the properties of the NS, such as mass, radius, moment of inertia, ellipticity of the NS, etc. It has been proposed that 4U 1728-34 and 4U 1820-30 could be possible candidates for dual-band GW sources, being potentially detectable by aLIGO and LISA simultaneously (see Suvorov 2021).

In addition to the GW emission, UCXBs are important multi-messenger systems. Active mass-transfer powers persistent X-ray and often optical radiation from both the accretion flow and the irradiated donor star, while systems that terminate mass-transfer can re-emerge as radio MSPs if the mass-

accretors are NSs. The combination of GW and electromagnetic observations provides complementary constraints on their orbital evolution and long-term accretion history.

8.2. Binary Evolution and NS Physics

Studies of UCXBs provide important constraints on key aspects of binary evolution, including the CE evolution, angular-momentum loss (e.g., MB), mass-transfer process, etc. (see, e.g., Nelemans & Jonker 2010; Lin & Yu 2018; Chen et al. 2021; Tauris & van den Heuvel 2023; Yang & Li 2024). They also offer valuable insights into NS physics, particularly the spin evolution and the maximum stable masses for NSs (see, e.g., Tauris et al. 2012; Kiziltan et al. 2013; Alsing et al. 2018).

UCXBs are thought to originate from close binaries that have undergone one or two CE phases (see Figures 1, 3 and 7). The CE phase is essential for shrinking the orbital separation from stellar scales to periods of order hours or less, thereby enabling the subsequent evolution toward the ultra-compact scale. Thus, their orbital period distribution and donor masses provide valuable empirical constraints and tests for the CE theory. In formation channels involving LMXBs, angular-momentum loss prior to the ultra-compact phase plays a critical role. In particular, MB together with GW radiation governs the secular orbital shrinkage before and during RLOF. Istrate et al. (2014) showed that under conventional MB prescriptions, it requires extreme fine-tuning of the initial donor mass and orbital period to form an UCXB from a detached MSP progenitor, leading to a very narrow parameter space. Subsequent studies demonstrated that the apparent fine-tuning issue is closely linked to an incomplete understanding of MB laws (see, e.g., Chen et al. 2021; Deng et al. 2021). Alternative MB prescriptions or reduced efficiencies can significantly broaden the viable parameter space, highlighting UCXBs as sensitive probes of angular-momentum loss mechanisms in low-mass binaries.

Most UCXBs host NSs with millisecond spin periods and very low-mass companions, indicating long duration and stable mass-transfer (see, e.g., Alpar et al. 1982; Bhattacharya & van den Heuvel 1991; Armas Padilla et al. 2023). The long-term accretion phase naturally spins up the NS to millisecond periods and may substantially increase its mass, establishing a direct evolutionary connection between UCXBs and radio MSPs. The high incidence of accreting MSPs among UCXBs reinforces this link. Because sustained accretion can push NSs toward their maximum mass, UCXBs offer a potential avenue to constrain the NS equation of state (see, e.g., Kiziltan et al. 2013; Alsing et al. 2018). Moreover, the observed ratio between NS and BH accretors in ultra-compact systems provides important information on the high-mass end of the initial mass function of stars.

Observational evidence indicates enrichment in different elements (e.g., He, C, O, Ne), implying diversity in the chemical composition of the donor stars (see Juett et al. 2001; Koliopanos et al. 2021). The composition influences thermonuclear burst properties, thus offering an additional diagnostic of donor structure (see Cumming et al. 2001). Explaining the observed chemical diversity requires donor stars that have reached different stages of nuclear burning and degrees of degeneracy, pointing to multiple formation pathways for UCXBs (see, e.g., Yungelson et al. 2002; Nelemans & Jonker 2010; Sengar et al. 2017; Chen et al. 2020; Wang et al. 2021).

9. Summary and Perspective

So far, about 50 UCXB candidates have been discovered, among which 22 UCXBs have been confirmed with high confidence. It has been suggested that most UCXBs may contain NS accretors, whereas three sources have been proposed to be BH-UCXB candidates though their nature is still undetermined. UCXBs play an important role in broad aspects of astrophysics. They are expected to be promising sources of low-frequency GWs. Their extremely short orbital periods place them in the mHz band, making them potential targets for space-based GW detectors such as LISA, TianQin and Taiji.

Currently, there are four evolutionary pathways that can lead to the formation of UCXBs, in which the WD donor channel is the main way for producing UCXBs. It remains uncertain for several key physical processes involved in the formation and evolution of UCXBs. In particular, the efficiency of MB in low-mass donors is still not well constrained, and different prescriptions for magnetic stellar winds can lead to significantly different orbital evolution and UCXB formation rates. Another important uncertainty concerns the stability of mass-transfer in NS+WD binaries, depending sensitively on the structure of the mass-donor. It also depends on the treatment of mass and angular momentum loss, including processes associated with the accretion disk such as disk winds and disk–orbit interactions. These uncertainties in binary evolution modeling continue to limit robust predictions of the formation channels and population properties of UCXBs. It is worth noting that the detection of UCXBs through GWs will provide independent constraints on their orbital evolution and help to further test models of compact binary evolution.

Meanwhile, the chemical composition of UCXB donors remains a major unresolved issue and serves as key evidence for distinguishing among different formation channels. Distinct evolutionary pathways are expected to produce different surface element abundance (see, e.g., Yungelson et al. 2002; Nelemans et al. 2010). For example, the presence of ^{22}Ne in the accretion disks of some UCXBs has been interpreted as

possible evidence for the origin of the AIC channel. Recently, Zhang et al. (2025) reported the observations of the BW system PSR J2322–2650 using the James Webb Space Telescope (JWST). This system has been suggested to originate from a UCXB with the He star donor channel (see Guo et al. 2022). The observations reveal an extremely carbon-enriched atmosphere in the companion, with anomalously high C/O and C/N ratios. These findings pose challenges to existing formation models, implying that the current formation channel may require additional physical processes to fully account for such abundances. At present, the observational constraints on the chemical composition of mass-donors in UCXBs remain very limited, but will be greatly improved by future high-sensitivity, multiwavelength spectroscopic observations with the ongoing and next-generation large-aperture telescopes and advanced X-ray facilities, such as JWST (see Gardner et al. 2006), the Chinese Space Station Survey Telescope (see CSST Collaboration et al. 2026), the planned Extremely Large Telescopes (ELTs), the Einstein Probe mission (see Yuan et al. 2025), Athena (see Nandra et al. 2013), Lynx (see Gaskin et al. 2019), etc. Such efforts will enable systematic measurements of elemental abundances and help to understand the diverse formation pathways of UCXBs.

Additionally, the nature of the mass-accretors plays a crucial role in understanding the origin of UCXBs. To date, nearly all confirmed UCXBs host NSs as the mass-accretors. Most of them are accreting millisecond X-ray pulsars with spin periods in the millisecond range, indicating that they have undergone prolonged mass-transfer and have been efficiently spun up through mass-accretion. Nevertheless, systems containing more slowly rotating NSs also exist. For example, 4U 1626–67 hosts a relatively slowly spinning NS (7.68 s) and has been suggested to originate from the AIC channel. Alternatively, the accretors in UCXBs can also be BHs. Radio continuum observations provide a powerful tool for identifying BH accretors in UCXBs. In particular, Miller-Jones et al. (2015) proposed that 47 Tuc X9 is a strong BH-UCXB candidate based on its consistency with the radio/X-ray correlation for accreting BHs. Its location in the orbital period–luminosity diagram further supports this interpretation (see Figure 10). Future high-sensitivity radio facilities, such as the Next Generation Very Large Array (ngVLA) and the Square Kilometre Array (SKA), will probe the radio properties of UCXBs to much deeper limits, potentially revealing hidden BH-UCXBs and better constraining their formation and evolution. In the future, multi-wavelength observations of UCXBs are required, along with more samples of such sources and further theoretical simulations.

Acknowledgments

This study is supported by the National Natural Science Foundation of China (NSFC, grant Nos 12225304, 12288102, 12273014, 12333008, 12422305 and 12403035), the CAS Project for Young Scientists in Basic Research (YSBR-148), the National Key R&D Program of China (No. 2021YFA1600404), the Yunnan Revitalization Talent Support Program (Young Talent Project and Yunling Scholar Project), the Yunnan Fundamental Research Project (Nos 202501AS070005 and 202605AS350010), and the International Centre of Supernovae (ICESUN), Yunnan Key Laboratory of Supernova Research (No. 202505AV340004).

ORCID iDs

Bo Wang https://orcid.org/0000-0002-3231-1167

References

Abbott, B. P., Abbott, R., Abbott, T. D., et al. 2016, PhRvL, 116, 061102
Abbott, B. P., Abbott, R., Abbott, T. D., et al. 2017, PhRvL, 119, 161101
Ablimit, I. 2019, ApJ, 881, 72
Alpar, M. A., Cheng, A. F., Ruderman, M. A., & Shaham, J. 1982, Natur, 300, 728
Alsing, J., Silva, H. O., & Berti, E. 2018, MNRAS, 478, 1377
Amaro-Seoane, P., Audley, H., Babak, S., et al. 2017, arXiv:1702.00786
Amaro-Seoane, P., Andrews, J., Arca Sedda, M., et al. 2023, LRR, 26, 2
Armas Padilla, M., Corral-Santana, J. M., Borghese, A., et al. 2023, A&A, 677, A186
Avakyan, A., Neumann, M., Zainab, A., et al. 2023, A&A, 675, A199
Bahramian, A., Heinke, C. O., Tudor, V., et al. 2017, MNRAS, 467, 2199
Bailyn, C. D., & Grindlay, J. E. 1987, ApJL, 316, L25
Bao, J., Shi, C., Wang, H., et al. 2019, PhRvD, 100, 084024
Batziou, E., Glas, R., Janka, H.-T., et al. 2025, ApJ, 984, 197
Belczynski, K., & Taam, R. E. 2004, ApJ, 603, 690
Benvenuto, O. G., De Vito, M. A., & Horvath, J. E. 2014, ApJL, 786, L7
Benvenuto, O. G., & Horvath, J. E. 2026, A&A, 705, L6
Bhattacharya, D., & van den Heuvel, E. P. J. 1991, PhR, 203, 1
Bildsten, L. 1998, ApJL, 501, L89
Bobrick, A., Davies, M. B., & Church, R. P. 2017, MNRAS, 467, 3556
Boyles, J., Lorimer, D. R., Turk, P. J., et al. 2011, ApJ, 742, 51
Brooks, J., Schwab, J., Bildsten, L., Quataert, E., & Paxton, B. 2017a, ApJ, 843, 151
Brooks, J., Schwab, J., Bildsten, L., et al. 2017b, ApJ, 850, 127
Canal, R., Isern, J., & Labay, J. 1990, ARA&A, 28, 183
Cartwright, T. F., Engel, M. C., Heinke, C. O., et al. 2013, ApJ, 768, 183
Casares, J., Jonker, P. G., & Israelian, G. 2017, in Handbook of Supernovae, ed. A. W. Alsabti & P. Murdin (Springer International Publishing AG), 1499
Chen, H.-L., Chen, X., & Han, Z. 2022a, ApJ, 935, 9
Chen, H.-L., Chen, X., Tauris, T. M., & Han, Z. 2013, ApJ, 775, 27
Chen, H.-L., Tauris, T. M., Chen, X., & Han, Z. 2022b, ApJ, 930, 134
Chen, H.-L., Tauris, T. M., Chen, X., & Han, Z. 2023, ApJ, 951, 91
Chen, H.-L., Tauris, T. M., Han, Z., & Chen, X. 2021, MNRAS, 503, 3540
Chen, M., & Liu, J. 2025, ApJ, 981, 175
Chen, W.-C. 2021, PhRvD, 103, 103004
Chen, W.-C., & Li, X.-D. 2006, MNRAS, 373, 305
Chen, W.-C., Liu, D.-D., & Wang, B. 2020, ApJL, 900, L8
Chen, W.-C., Liu, X.-W., Xu, R.-X., & Li, X.-D. 2011, MNRAS, 410, 1441
Chen, W.-C., & Podsiadlowski, P. 2016, ApJ, 830, 131
Chou, Y., & Grindlay, J. E. 2001, ApJ, 563, 934
Coti Zelati, F., de Ugarte Postigo, A., Russell, T. D., et al. 2021, A&A, 650, A69
CSST Collaboration, Gong, Y., Miao, H., et al. 2026, SCPMA, 69, 239501
Cumming, A. 2003, ApJ, 595, 1077
Cumming, A., Zweibel, E., & Bildsten, L. 2001, ApJ, 557, 958
Dage, K. C., Bahramian, A., Naoz, S., et al. 2024, MNRAS, 529, 1347
Davies, M. B., Benz, W., & Hills, J. G. 1992, ApJ, 401, 246
Davies, M. B., & Hansen, B. M. S. 1998, MNRAS, 301, 15

Deloye, C. J., & Bildsten, L. 2003, ApJ, 598, 1217
Deng, Z.-L., & Li, X.-D. 2024, ApJ, 971, 54
Deng, Z.-L., Li, X.-D., Gao, Z.-F., & Shao, Y. 2021, ApJ, 909, 174
Deng, Z.-L., Li, X.-D., Shao, Y., Mao, Y.-H., & Jiang, L. 2025, A&A, 704, A2
Dessart, L., Burrows, A., Livne, E., & Ott, C. D. 2007, ApJ, 669, 585
Ergma, E. 1996, A&A, 315, L17
Falcke, H., & Rezzolla, L. 2014, A&A, 562, A137
Fryer, C., Benz, W., Herant, M., & Colgate, S. A. 1999, ApJ, 516, 892
Galloway, D. K., Muno, M. P., Hartman, J. M., Psaltis, D., & Chakrabarty, D. 2008, ApJS, 179, 360
Gardner, J. P., Mather, J. C., Clampin, M., et al. 2006, SSRv, 123, 485
Gaskin, J. A., Swartz, D. A., Vikhlinin, A., et al. 2019, JATIS, 5, 021001
Ginzburg, S., & Quataert, E. 2020, MNRAS, 495, 3656
Green, M. J., van Roestel, J., Wong, T. L. S., et al. 2025, A&A, 700, A107
Gu, W.-M., Yi, T., & Liu, T. 2020, MNRAS, 497, 1543
Guo, Y.-L., Wang, B., Chen, W.-C., et al. 2024a, MNRAS, 530, 4461
Guo, Y.-L., Wang, B., & Han, Z.-W. 2022, MNRAS, 515, 2725
Guo, Y.-L., Wang, B., & Li, X. 2024b, MNRAS, 527, 7394
Guo, Y.-L., Wang, B., Li, X., Liu, D., & Tang, W. 2025, ApJ, 992, 144
Guo, Y.-L., Wang, B., Wu, C.-Y., et al. 2023, MNRAS, 526, 932
Han, J. L., Wang, C., Wang, P. F., et al. 2021, RAA, 21, 107
Han, Z., Podsiadlowski, P., Maxted, P. F. L., Marsh, T. R., & Ivanova, N. 2002, MNRAS, 336, 449
Han, Z.-W., Ge, H.-W., Chen, X.-F., & Chen, H.-L. 2020, RAA, 20, 161
He, J.-G., Shao, Y., Xu, X.-J., & Li, X.-D. 2024, MNRAS, 529, 1886
Heinke, C. O., Ivanova, N., Engel, M. C., et al. 2013, ApJ, 768, 184
Hernández Santisteban, J. V., Cúneo, V., Degenaar, N., et al. 2019, MNRAS, 488, 4596
Horiuchi, S., Nakamura, K., Takiwaki, T., Kotake, K., & Tanaka, M. 2014, MNRAS, 445, L99
Huang, S.-J., Hu, Y.-M., Korol, V., et al. 2020, PhRvD, 102, 063021
Iben, I., Jr., Tutukov, A. V., & Yungelson, L. R. 1995, ApJS, 100, 233
in't Zand, J. J. M., Jonker, P. G., & Markwardt, C. B. 2007, A&A, 465, 953
Istrate, A. G., Tauris, T. M., Langer, N., et al. 2014, A&A, 571, A45
Ivanova, N., Heinke, C. O., Rasio, F. A., Belczynski, K., & Fregeau, J. M. 2008, MNRAS, 386, 553
Ivanova, N., Rasio, F. A., Lombardi, J. C., Jr., Dooley, K. L., & Proulx, Z. F. 2005, ApJL, 621, L109
Jiang, L., Chen, W.-C., & Li, X.-D. 2017, ApJ, 837, 64
Juett, A. M., Psaltis, D., & Chakrabarty, D. 2001, ApJL, 560, L59
Justham, S., Rappaport, S., & Podsiadlowski, P. 2006, MNRAS, 366, 1415
Kalogera, V. 1999, ApJ, 521, 723
Kang, Y., Zhu, J.-P., Shao, L., et al. 2026, A&A, 706, A106
Kiziltan, B., Kottas, A., De Yoreo, M., & Thorsett, S. E. 2013, ApJ, 778, 66
Kluzniak, W., Ruderman, M., Shaham, J., & Tavani, M. 1988, Natur, 334, 225
Koliopanos, F., Péault, M., Vasilopoulos, G., & Webb, N. 2021, MNRAS, 501, 548
Kozai, Y. 1962, AJ, 67, 591
Kruckow, M. U., Tauris, T. M., Langer, N., et al. 2016, A&A, 596, A58
Lee, U. 2014, MNRAS, 442, 3037
Li, E.-K., Liu, S., Torres-Orjuela, A., et al. 2025a, RPPh, 88, 056901
Li, K. J., Long, J. S., Wu, K., & Kong, A. K. H. 2025b, ApJ, 984, 41
Li, L., Wang, B., Liu, D., et al. 2024, MNRAS, 534, 3400
Li, X.-D. 2002, ApJ, 564, 930
Li, X.-D. 2020, RAA, 20, 162
Li, Z., & Chen, X. 2024, ResPh, 59, 107568
Lidov, M. L. 1962, Planet. Space Sci., 9, 719
Lin, J., Rappaport, S., Podsiadlowski, P., et al. 2011, ApJ, 732, 70
Lin, J., & Yu, W. 2018, MNRAS, 474, 1922
Liu, D., & Wang, B. 2020, MNRAS, 494, 3422
Liu, D., & Wang, B. 2023, MNRAS, 521, 6053
Liu, D., Wang, B., Chen, W., Zuo, Z., & Han, Z. 2018, MNRAS, 477, 384
Liu, Q. Z., van Paradijs, J., van den Heuvel, E. P. J., et al. 2007, A&A, 469, 807
Liu, W.-M., Jiang, L., & Chen, W.-C. 2021, ApJ, 910, 22
Lü, G., Zhu, C., Wang, Z., & Iminniyaz, H. 2017, ApJ, 847, 62
Luo, J., Chen, L.-S., Duan, H.-Z., et al. 2016, CQGra, 33, 035010
Ma, B., & Li, X.-D. 2009a, ApJ, 698, 1907
Ma, B., & Li, X.-D. 2009b, ApJ, 691, 1611
Ma, Q.-Q., Zhang, J., Gu, W.-M., et al. 2026, Innov, 7, 101181
Manchester, R. N., Hobbs, G. B., Teoh, A., & Hobbs, M. 2005, AJ, 129, 1993
Markwardt, C. B., Swank, J. H., Strohmayer, T. E., in 't Zand, J. J. M., & Marshall, F. E. 2002, ApJL, 575, L21
Meng, X.-C. 2025, arXiv:2505.18702
Miller-Jones, J. C. A., Strader, J., Heinke, C. O., et al. 2015, MNRAS, 453, 3918
Moutard, D. L., Ludlam, R. M., Sudha, M., et al. 2024, ApJ, 968, 51
Nandra, K., Barret, D., Barcons, X., et al. 2013, arXiv:1306.2307
Narayan, R., & Yi, I. 1995, ApJ, 452, 710
Nelemans, G. 2009, CQGra, 26, 094030
Nelemans, G., & Jonker, P. G. 2010, NewAR, 54, 87
Nelemans, G., Jonker, P. G., Marsh, T. R., & van der Klis, M. 2004, MNRAS, 348, L7
Nelemans, G., Jonker, P. G., & Steeghs, D. 2006, MNRAS, 370, 255
Nelemans, G., Yungelson, L. R., van der Sluys, M. V., & Tout, C. A. 2010, MNRAS, 401, 1347
Nelson, L. A., Rappaport, S. A., & Joss, P. C. 1986, ApJ, 304, 231
Ng, M., Ray, P. S., Bult, P., et al. 2021, ApJL, 908, L15
Nomoto, K., & Kondo, Y. 1991, ApJL, 367, L19
Nomoto, K., Miyaji, S., Sugimoto, D., & Yokoi, K. 1979, in IAU Colloq. 53: White Dwarfs and Variable Degenerate Stars, ed. H. M. van Horn, V. Weidemann, & M. P. Savedoff, 56
O'Connor, E., & Ott, C. D. 2011, ApJ, 730, 70
Pan, Z., Lu, J. G., Jiang, P., et al. 2023, Natur, 620, 961
Paschalidis, V., MacLeod, M., Baumgarte, T. W., & Shapiro, S. L. 2009, PhRvD, 80, 024006
Peuten, M., Brockamp, M., Küpper, A. H. W., & Kroupa, P. 2014, ApJ, 795, 116
Podsiadlowski, P., Han, Z., & Rappaport, S. 2003a, MNRAS, 340, 1214
Podsiadlowski, P., Rappaport, S., & Han, Z. 2003b, MNRAS, 341, 385
Podsiadlowski, P., Rappaport, S., & Pfahl, E. D. 2002, ApJ, 565, 1107
Portegies Zwart, S. F., Verbunt, F., & Ergma, E. 1997, A&A, 321, 207
Pringle, J. E., & Webbink, R. F. 1975, MNRAS, 172, 493
Pylyser, E. H. P., & Savonije, G. J. 1989, A&A, 208, 52
Pylyser, E., & Savonije, G. J. 1988, A&A, 191, 57
Qin, K., & Chen, W.-C. 2024, ApJ, 971, 57
Qin, K., Jiang, L., & Chen, W.-C. 2023, ApJ, 944, 83
Qin, K., Xu, K., Liu, D.-D., et al. 2024, ApJ, 961, 110
Rappaport, S., Joss, P. C., & Webbink, R. F. 1982, ApJ, 254, 616
Rappaport, S., Verbunt, F., & Joss, P. C. 1983, ApJ, 275, 713
Roberts, M. S. E. 2013, IAUS, 291, 127
Ruan, W.-H., Liu, C., Guo, Z.-K., Wu, Y.-L., & Cai, R.-G. 2020, NatAs, 4, 108
Ruan, W.-H., Liu, C., Guo, Z.-K., Wu, Y.-L., & Cai, R.-G. 2021, Resea, 2021, 6014164
Ruderman, M., Shaham, J., & Tavani, M. 1989, ApJ, 336, 507
Ruiter, A. J., Ferrario, L., Belczynski, K., et al. 2019, MNRAS, 484, 698
Ruiter, A. J., & Seitenzahl, I. R. 2025, A&ARv, 33, 1
Sanna, A., Bahramian, A., Bozzo, E., et al. 2018, A&A, 610, L2
Sanna, A., Bult, P., Ng, M., et al. 2022, MNRAS, 516, L76
Sanna, A., Papitto, A., Burderi, L., et al. 2017, A&A, 598, A34
Sansom, A. E., Watson, M. G., Makishima, K., & Dotani, T. 1989, PASJ, 41, 591
Savonije, G. J., de Kool, M., & van den Heuvel, E. P. J. 1986, A&A, 155, 51
Sazonov, S., Paizis, A., Bazzano, A., et al. 2020, NewAR, 88, 101536
Sengar, R., Tauris, T. M., Langer, N., & Istrate, A. G. 2017, MNRAS, 470, L6
Shao, Y., & Li, X.-D. 2012, ApJ, 756, 85
Shao, Y., & Li, X.-D. 2015, ApJ, 809, 99
Solheim, J. E. 2010, PASP, 122, 1133
Steele, M. M., Zepf, S. E., Maccarone, T. J., et al. 2014, ApJ, 785, 147
Strohmayer, T., & Mahmoodifar, S. 2014, ApJ, 784, 72
Suvorov, A. G. 2021, MNRAS, 503, 5495
Taam, R. E., & van den Heuvel, E. P. J. 1986, ApJ, 305, 235
Tauris, T. M. 2018, PhRvL, 121, 131105
Tauris, T. M., Langer, N., & Kramer, M. 2012, MNRAS, 425, 1601
Tauris, T. M., Sanyal, D., Yoon, S. C., & Langer, N. 2013, A&A, 558, A39
Tauris, T. M., & Savonije, G. J. 1999, A&A, 350, 928
Tauris, T. M., & van den Heuvel, E. P. J. 2023, Physics of Binary Star Evolution. From Stars to X-Ray Binaries and Gravitational Wave Sources (Princeton Univ. Press)

Toonen, S., Perets, H. B., Igoshev, A. P., Michaely, E., & Zenati, Y. 2018, A&A, 619, A53
Tudor, V., Miller-Jones, J. C. A., Knigge, C., et al. 2018, MNRAS, 476, 1889
van den Heuvel, E. P. J., & van Paradijs, J. 1988, Natur, 334, 227
van der Sluys, M. V., Verbunt, F., & Pols, O. R. 2005a, A&A, 431, 647
van der Sluys, M. V., Verbunt, F., & Pols, O. R. 2005b, A&A, 440, 973
van Haaften, L. M., Nelemans, G., Voss, R., & Jonker, P. G. 2012a, A&A, 541, A22
van Haaften, L. M., Nelemans, G., Voss, R., Wood, M. A., & Kuijpers, J. 2012b, A&A, 537, A104
van Haaften, L. M., Voss, R., & Nelemans, G. 2012c, A&A, 543, A121
Van, K. X., Ivanova, N., & Heinke, C. O. 2019, MNRAS, 483, 5595
Verbunt, F. 1987, ApJL, 312, L23
Verbunt, F. 2005, AIPC, 797, 30
Verbunt, F., & Rappaport, S. 1988, ApJ, 332, 193
Vleeschower, L., Corongiu, A., Stappers, B. W., et al. 2024, MNRAS, 530, 1436
Voss, R., & Gilfanov, M. 2007, MNRAS, 380, 1685
Wang, B. 2018, MNRAS, 481, 439
Wang, B., Chen, W.-C., Liu, D.-D., et al. 2021, MNRAS, 506, 4654
Wang, B., & Liu, D. 2020, RAA, 20, 135
Wang, B., Liu, D., & Chen, H. 2022, MNRAS, 510, 6011
Wang, B., Liu, D., Guo, Y., & Han, Z. 2026, RAA, 26, 032001
Wang, B., Podsiadlowski, P., & Han, Z. 2017, MNRAS, 472, 1593
Wang, C., Jia, K., & Li, X.-D. 2016, MNRAS, 457, 1015
Warner, B. 1995, Ap&SS, 225, 249
Watarai, K.-y., Mizuno, T., & Mineshige, S. 2001, ApJL, 549, L77
Woosley, S. E., & Baron, E. 1992, ApJ, 391, 228
Wu, C., Wang, B., & Liu, D. 2019, MNRAS, 483, 263
Wu, C., Xiong, H., Han, Z., & Wang, B. 2023a, MNRAS, 525, 6295
Wu, C., Xiong, H., Lin, J., et al. 2023b, ApJL, 944, L54
Xu, X.-J., & Li, X.-D. 2007, A&A, 476, 1283
Xuan, Z., Shariat, C., & Naoz, S. 2025, ApJ, 995, 27
Yang, H.-R., & Li, X.-D. 2024, ApJ, 974, 298
Yang, X.-P., & Chen, W.-C. 2025, ApJ, 995, 99
Yang, X.-P., Xu, K., Gao, Z.-F., Jiang, L., & Chen, W.-C. 2025a, ApJ, 986, 219
Yang, Z. L., Han, J. L., Jing, W. C., & Su, W. Q. 2023, ApJL, 956, L39
Yang, Z. L., Han, J. L., Zhou, D. J., et al. 2025b, Sci, 388, 859
Yu, S., Lu, Y., & Jeffery, C. S. 2021, MNRAS, 503, 2776
Yu, S., Lu, Y., Jeffery, C. S., et al. 2026a, MNRAS, 545, staf2077
Yu, W., Pala, A. F., Kupfer, T., et al. 2026b, A&A, 706, A14
Yuan, W., Dai, L., Feng, H., et al. 2025, SCPMA, 68, 239501
Yungelson, L. R., Nelemans, G., & van den Heuvel, E. P. J. 2002, A&A, 388, 546
Zhang, J., Bao, T., & Li, Z. 2024a, MNRAS, 530, 2096
Zhang, M., Beleznay, M., Brandt, T. D., et al. 2025, ApJL, 995, L64
Zhang, Z., Wu, C., Aryan, A., et al. 2024b, ApJ, 975, 186
Zhu, C.-H., Lü, G.-L., & Wang, Z.-J. 2012, RAA, 12, 1526